

**Head Movements of Children in MEG: Quantification, Effects on
Source Estimation, and Compensation**

by

Daniel T. Wehner

B.S.E., Biomedical Engineering
University of Iowa, 2000

Submitted to the Department of Electrical Engineering and Computer Science
in partial fulfillment of the requirements for the degree of

Master of Science in Electrical Engineering and Computer Science
at the
MASSACHUSETTS INSTITUTE OF TECHNOLOGY

June 2007

© 2007 Daniel T. Wehner, MMVII. All rights reserved

The author hereby grants to MIT permission to reproduce and distribute publicly
paper and electronic copies of this thesis document in whole or in part.

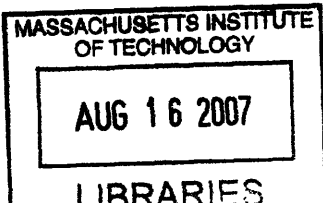
Signature of Author
Department of Electrical Engineering and Computer Science
10 May 2007

Certified by
Elfar Adalsteinsson
R.J. Shillman Assistant Professor of EECS and HST
Thesis Supervisor

Certified by
Seppo Ahlfors
Assistant Professor of Radiology, Harvard Medical School
Thesis Co-Supervisor

Certified by
Matti Hämäläinen
Associate Professor of Radiology, Harvard Medical School
Thesis Co-Supervisor

Accepted by
Arthur C. Smith
Professor of Electrical Engineering
Chairman, Department Committee on Graduate Theses



ARCHIVES

Head Movements of Children in MEG: Quantification, Effects on Source Estimation, and Compensation

by

Daniel T. Wehner

Submitted to the Department of Electrical Engineering and Computer Science
on May 11, 2007 in Partial Fulfillment of the
Requirements for the Degree of Master of Science in
Electrical Engineering and Computer Science

Abstract

Head movements during MEG recordings in children may lead to inaccurate localization of brain activity. In this thesis, we examined the effects of head movements on source estimation in twenty children performing a simple auditory cognitive task. In addition, we tested the ability of a recently introduced spherical harmonic expansion method, signal space separation (SSS), to compensate for the effects of head movements on two source models: equivalent current dipoles (ECDs) and minimum norm estimates (MNE). In the majority of subjects, the goodness-of-fit of ECDs fit to the peak of the auditory N100m response was increased following the SSS correction compared with the averaged forward solution method proposed earlier. The spatial spread of ECDs as determined with a bootstrapping approach was also reduced after SSS correction. In addition, the MNE source estimates were spatially sharpened following SSS application, indicative of an increase in signal to noise ratio. Together these results suggest that SSS is an effective method to compensate for head movements in MEG recordings in children.

Thesis Supervisor 1: Elfar Adalsteinsson, Ph.D.

Title: Assistant Professor of EECS and HST

Thesis Supervisor 2: Seppo Ahlfors, Ph.D.

Title: Assistant Professor of Radiology, Harvard Medical School

Thesis Supervisor 3: Matti Hämäläinen, Ph.D.

Title: Associate Professor of Radiology, Harvard Medical School

Acknowledgments

It has been a rather circuitous route that led me to this masters project. With a background in Biomedical Engineering, I decided six years ago to take a stroll through the somewhat nebulous world of pediatric cognitive neuroscience. At several points along the path, interesting branches appeared which could only be navigated via a merging of technical knowledge and practical experience with conducting imaging experiments with children. The work in this thesis represents one of those branches, as I travel back into the familiar land of complex equations, engineering, and physics.

First I would like to thank my triumvirate of supervisors, Seppo Ahlfors, Matti Hämäläinen, and Elfar Adalsteinsson. This project would not have been possible if it were not for your patience and wisdom that you have provided to me over the past few years.

I want to thank all of my many coworkers at the Athinoula A. Martinos Center for Biomedical Imaging. I especially would like to thank Maria Mody, my PhD thesis supervisor, for helping with various aspects of the project. Surina Basho, Deirdre von Pechmann and Dan Wakeman have helped out tremendously in assisting with the MEG recordings.

I would also like to thank all of my colleagues over in Finland who have provided assistance to this project including Jukka Nenonen and Samu Taulu and everyone else at Elekta-Neuromag.

To Asa Masaki, thanks for putting up with the late nights and the long weekends that working on two theses at once yields. Without your continued support and encouragement, everything in my life would be so much more difficult.

I would also like to thank all the children and parents for their willingness to participate in the studies in this thesis.

And finally, to my dad...your hard work and dedication to engineering has been an inspiration to me all of my life. I dedicate this thesis in your honor.

This work has been supported in part by several grants from the NIH (DC00159, HD056355), the National Center for Research Resources (P41RR14075), and the Mental Illness and Neuroscience Discovery (MIND) Institute. Additional funding was from an NIH Training Grant (DC00038) and an NIH Neuroimaging Training Program Fellowship (5T32EB001680; PI: Bruce Rosen).

List of Figures

2.1 Neurophysiological basis of the MEG signal.....	4
2.2 The Elekta-Neuromag 306-channel MEG system.....	6
2.3 Equivalent Current Dipole (ECD) and Minimum Norm Estimate (MNE) source modeling.....	7
2.4 Head position within MEG sensor array.....	9
3.1 The coordinate system for the MEG measurements.....	13
4.1 Head movement statistics in one child.....	23
4.2 Dipole source localization errors.....	26
4.3 Event-related magnetic fields for one child.....	28
4.4 Distributed source estimates in one child.....	30
4.5 SSS compensation and MNE.....	31

Contents

1	Introduction.....	1
1.1	Motivation.....	1
1.2	Outline of the thesis.....	1
1.3	Thesis contributions.....	2
2	Background.....	4
2.1	Neurophysiological basis of the MEG signal.....	4
2.2	MEG data acquisition and analysis.....	5
2.3	MEG recordings in children.....	7
2.4	Continuous head localization.....	9
2.5	Movement compensation.....	10
3	Methods.....	12
3.1	Quantitative assessment of head movement in children.....	12
3.2	Dipole localization error due to head movements.....	15
3.3	Movement compensation using the Signal Space Separation method.....	16
4	Results and Discussion.....	22
4.1	Quantitative assessment of head movement in children.....	22
4.2	Dipole localization error due to head movements.....	24
4.3	Movement compensation using the Signal Space Separation method.....	27
4.3.1	Equivalent Current Dipoles.....	29
4.3.2	Minimum Norm Estimates.....	30
4.4	Discussion.....	32
5	Conclusions.....	34
5.1	Summary.....	34
5.2	Future Work.....	35
	Bibliography.....	36

1. Introduction

1.1 Motivation

Magnetoencephalography (MEG), as a non-invasive technique to record evoked brain responses to cognitive processes in adults has been established for some time (Hämäläinen, Hari, Ilmoniemi, Knuutila, & Lounasmaa, 1993). In an evoked-response study, stimuli are presented repeatedly and the data are subsequently averaged over several trials, time locked to the stimulus. By averaging evoked responses in this manner, one typically assumes that the position of the head relative to the sensor array does not change throughout the recording session. However, this assumption is not necessarily valid, particularly when recording from children. We examined the effects of head movements on source estimation in twenty children performing a simple auditory cognitive task. In addition, we tested the ability of a recently introduced spherical harmonic expansion method, signal space separation (SSS), to compensate for the effect of these head movements on two source models: equivalent current dipoles (ECDs) and minimum norm estimates (MNE).

1.2 Outline of the thesis

Chapter 2 presents the relevant background on MEG signals and MEG recording techniques used with children. This chapter also describes existing methods for continuous head localization during MEG recordings and discusses previously described methods to compensate for the effects of head movement in MEG data.

Chapter 3 discusses the methodology that was used to quantify head movement, their effect on source estimates, and to evaluate the Signal Space Separation (SSS) method to compensate for these head movements.

Chapter 4 provides the results from the various analyses used in the thesis, and discusses possible implications of these results.

Chapter 5 includes a general overview of the results, summarizes the contributions of the thesis, and suggests possibilities for future work.

1.3 Thesis contributions

The experiments designed herein test the hypothesis that SSS is an effective method of compensating for head movements during recording of MEG data in children. To test this general hypothesis, we proposed the following aims:

- 1) Quantify the head motion of children during MEG recordings.** Data from head position indicator (HPI) coils was measured continuously as each subject listened to word stimuli. From these measured data, the translation and rotation of the subject's head was calculated every 200 ms and averaged into 10-second bins. The direction with the most movement was identified in each subject and compared across subjects.
- 2) Determine the effect of head movements on the accuracy of the estimated location of equivalent current dipoles (ECD) using simulations as well as auditory evoked MEG data.** We used dipole simulations to estimate the mean, and standard deviation of dipole localization errors that would have occurred if continuous head position information was not taken into account in the calculation of the forward solution.

3) Evaluate the effectiveness of SSS for compensating for the effects of head movements on MEG data in children. We compared the ECD location and goodness-of-fit for auditory N100m evoked responses with and without SSS correction to examine the effect of SSS on dipole localization. In addition, the impact of SSS on the quality of the data was quantified using the distributed minimum norm estimation (MNE) source model. Specifically, we examined the differences between the forward solutions in four cases using: the initial head position only, an average head position from the beginning of each run, SSS-correction transforming the data to the head position at the beginning of each run, and SSS-correction transforming the data to the head position at the beginning of the experiment. The difference between these cases was evaluated by calculating the mean MNE amplitude in a small cortical patch surrounding the MEG response at the peak latency of the N100m for each forward solution condition.

2. Background

2.1 Neurophysiological basis of MEG signal

MEG measures weak magnetic fields (on the order of 10^{-14} Tesla) arising from thousands of synchronously active neurons in the brain (Hämäläinen et al., 1993; Paetau, 2002; Sato, Balish, & Muratore, 1991). According to Maxwell's equations, a moving electric charge always generates a magnetic field oriented perpendicularly to the direction of the movement. The sources of MEG signals are thought to be post-synaptic currents within the apical dendrites of pyramidal neurons in the cerebral cortex (Fig. 2.1). These so called primary currents, \vec{j}^p , are oriented perpendicular to the cortical surface. Sources that are radial, that is oriented perpendicular to the skull surface, do not produce an appreciable magnetic field outside of the head; The percentage of sources that are strictly radial is small.

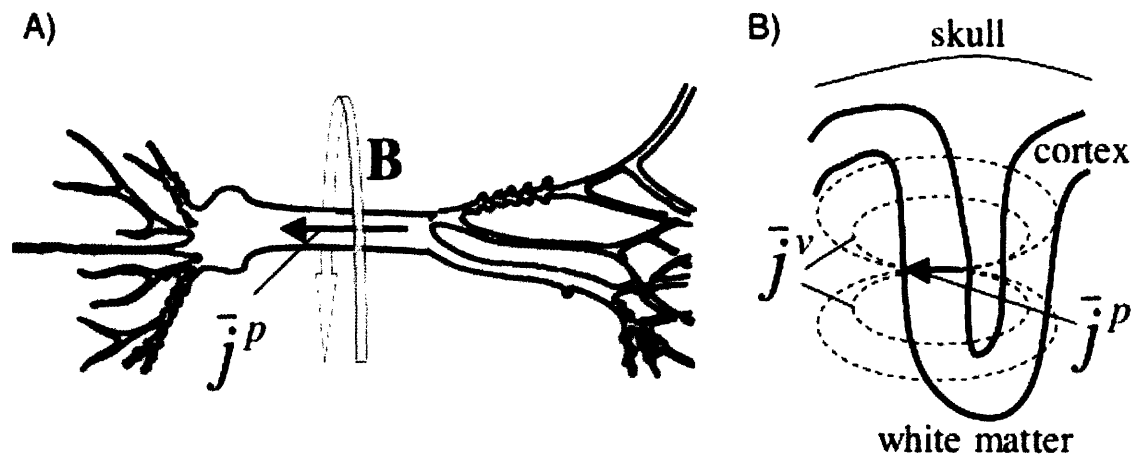


Figure 2.1: A) The intracellular current, \vec{j}^p , in an apical dendrite of a pyramidal cell surrounded with a surrounding magnetic field **B**. B) The externally recorded magnetic signals arise from the active primary currents (\vec{j}^p) as well as the associated passive (ohmic) volume currents (\vec{j}^v) [Adapted from Paetau, 2002].

2.2 MEG data acquisition and analysis

MEG signals from the brain are much smaller than the magnetic fields generated by external environmental sources. Hence, MEG measurements are usually carried out in a magnetically shielded room using sensitive detectors of magnetic flux called superconducting quantum interference devices (SQUIDs) (Zimmerman, Thiene, & Harding, 1970). The first MEG measurement of brain activity using a SQUID sensor was conducted at MIT (Cohen, 1972).

In modern whole-head MEG devices, several hundreds of sensors are immersed in a liquid helium dewar, which is helmet-shaped and encloses most of the head (Fig. 2.2A). This arrangement of MEG sensors allows for identification of simultaneous signals from multiple brain regions. The sensors are typically 3-4 cm from the cortical surface depending on the subject's head position. Most MEG systems are designed for use with adults. Hence, the distance between the MEG sensors and the cortical sources may be further in children with smaller head sizes. Each of the 102 sensor elements in the MEG device used in the present thesis (Fig. 2.2B: squares) contained one axial magnetometer and two orthogonally-oriented planar gradiometers. Gradiometers are differential sensors, which maximally detect signals from sources directly below the sensors, and are generally insensitive to sources far away from the sensors. In contrast, magnetometers are more sensitive to deep sources than gradiometers are.

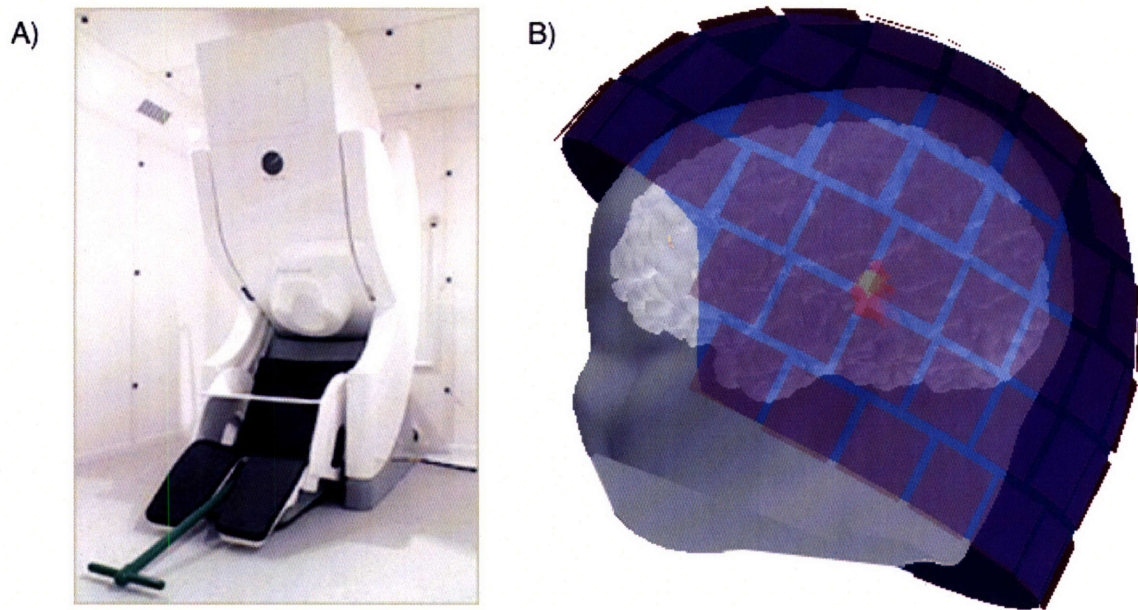


Figure 2.2: A) The Elekta-Neuromag™ 306-channel MEG device. B) The scalp surface for a child is shown within a representation of a helmet-shaped array of MEG sensor elements (purple squares). The scalp surface is transparent to reveal the estimated brain activation in the left superior temporal cortex.

MEG experiments are typically designed to examine either spontaneous activity, e.g., for detection of epileptic spikes, or evoked activity that is time-locked to the presentation of a stimulus (as in the present thesis). An important goal of MEG data analysis is to estimate the spatiotemporal distribution of the neural currents giving rise to the observed MEG signals by solving the ‘inverse problem’. The inverse problem is ill-posed as there are an infinite number of primary (source) current distributions that result in the same field pattern (Sarvas, 1987). Therefore, the brain sources must be appropriately modeled and additional constraints must be employed, e.g., obtained from

magnetic resonance imaging (MRI), to eliminate unrealistic solutions. An equivalent current dipole (ECD) is a good approximation for a small region of activated cortex (Fig. 2.3A). More complicated source configurations can be modeled using multi-dipole models. Alternatively, a distributed solution such as the minimum norm estimate (MNE) (Hämäläinen & Ilmoniemi, 1994), may provide a better approximation of widespread activation (Fig 2.3B). The location of an ECD or MNE activation can be viewed on a subject's MRI. Fiducial points on the head are usually digitized at the beginning of the experiment for alignment of the MEG data with the MRI.

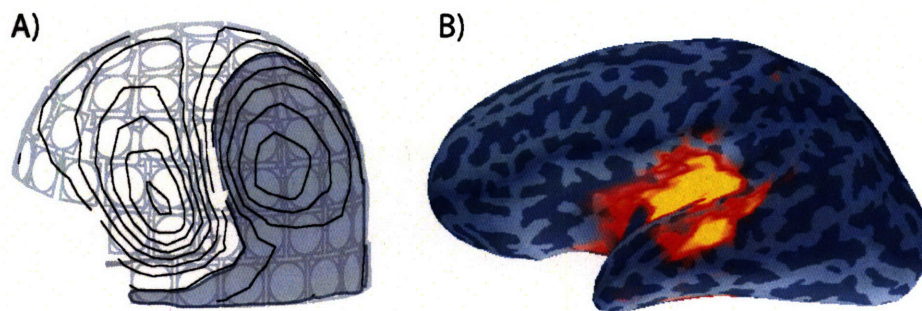


Figure 2.3: A) A magnetic field map for an equivalent current dipole (ECD) source located in the auditory cortex. B) Minimum norm estimate (MNE) for a distributed source in the superior temporal cortex.

2.3 MEG recordings in children

One limiting factor affecting the use of MEG in children is the low signal to noise ratio (SNR). Several factors contribute to the low SNR in children compared to adults; these include less focused attention during long recording sessions, more frequent eye movement and blink-related artifacts, and smaller head size (Phillips, 2005). Whereas the first two can be at least partially mitigated by means of engaging experimental

designs with detailed instructions, extensive training or practice, or with more frequent rest periods during the recording, smaller head size can only be dealt with by designing smaller MEG sensor arrays for use with children, or by the development of better signal processing methods to separate the small MEG signal from the background noise. For magnetometers and a dipolar current source, the strength of the MEG signal is inversely proportional to the square of the distance from the source to the sensor: for differential measures (gradiometers) the fall-off with distance is even faster. For children with small heads, this is particularly troublesome as the scalp may be several centimeters from some of the sensors depending on their head position inside of the measurement helmet containing the sensors (Fig. 2.4), resulting in very weak signals (Marinkovic, Cox, Reid, & Halgren, 2004). An additional problem with the small head size is that children often tend to move their heads considerably inside the measurement helmet during the experiment. This head movement, if not corrected for, leads to loss of spatial details and inaccurate localization of the brain sources of interest. Although several approaches have been employed to reduce head movements during MEG experiments, including the use of foam padding inside the helmet containing the sensors or the use of bite bars, many of these methods are uncomfortable for children and may result in poor task performance. However, such measures may not be required if the child's head position is monitored continuously during the measurement and this information can be used to align the magnetic fields at each measured time point to a virtual sensor array.

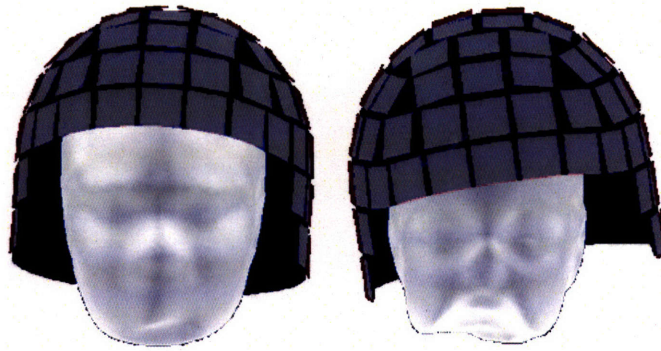


Figure 2.4: Head position within MEG sensor array. The scalp surface for an adult (left) and a child (right) subject is shown within a representation of a helmet-shaped array of MEG sensor elements (gray squares).

2.4 Continuous head localization

The relative position of the head with respect to the MEG sensor array can be determined with the help of three or more small coils that are attached to the head and fed with continuously oscillating currents during the measurement (Ahlfors & Ilmoniemi, 1989; Fuchs, Wischmann, Wagner, & Kruger, 1995; Incardona, Narici, Modena, & Erne, 1992). By using currents that are outside of the frequency range of the brain activity of interest, the magnetic field due to the coil currents can be filtered out of the data before analyzing the brain signals, allowing continuous acquisition of head localization data (de Munck, Verbunt, Van't Ent, & Van Dijk, 2001; Uutela, Taulu, & Hämäläinen, 2001; Wilson, 2004). Typically, the locations of the coils with respect to anatomical landmarks are determined with a 3D digitizer before the MEG recording. The required coordinate transform between the anatomy and MEG sensor array is achieved by extracting the coil

signal amplitudes and by using a least-square fit in which each coil is approximated as a magnetic dipole (Ahlfors & Ilmoniemi, 1989; Fuchs et al., 1995; Incardona et al., 1992).

2.5 Movement compensation

The sequence of the continuous head localization information can be used to compensate for effects of the head movement on the MEG data. The compensation effectively results extrapolation of the data to a virtual sensor array, which is fixed with respect to the subject's head. Two general approaches have been suggested: one is to use spherical harmonics expansion (Taulu & Kajola, 2004; Wilson, 2004), the other to construct a distributed source estimate (MNE) from which the measured data can be extrapolated to a standard representation (Burghoff, Nenonen, Trahms, & Katila, 2000; de Munck et al., 2001; Hämäläinen & Ilmoniemi, 1994; Numminen, Ahlfors, Ilmoniemi, Montonen, & Nenonen, 1995). In the latter approach, the calculations can become quite time consuming since a forward and inverse model needs to be constructed for each head position. The amount of calculations can be reduced by using series expansions in spherical harmonics (Taulu & Kajola, 2004; Wilson, 2004). Alternatively, the correction could be accomplished by averaging the original epochs as usual and by computing an average forward model over the different head positions (Uutela et al., 2001). In the signal-space separation (SSS) method the field patterns originating from outside a sphere encompassing the sensor array are separated from those originating from inside the head. Thus, SSS is a "hybrid" method of generating virtual channels: it uses spherical harmonics to obtain field patterns specifically generated by source distributions inside the head, but without constructing an explicit source estimate.

In this thesis we measured and quantified the head motion of children. We then examined the effect of this realistic head motion on equivalent current dipole (ECD) source estimates using simulation. Finally, we evaluated the effectiveness of the SSS method to compensate for the effect of head movements on ECD and minimum norm estimates (MNE).

3. Methods

3.1 Quantitative assessment of head movements in children

To assess the amount of head movement in children, we used data from an investigation of a cognitive task, the results of which are reported elsewhere (Wehner et al, submitted). Twenty children between 8-12 years of age participated in the study. The children had no history of neurological or psychological problems, and they had normal or corrected to normal vision, and normal hearing. All children had English as their primary language. Written informed assent/consent was obtained from all subjects/parents in accordance with the Human Subjects Committee at Massachusetts General Hospital and the Massachusetts Institute of Technology.

A typical protocol for collecting MEG data was used. MEG was recorded using a 306-channel (204 first-order planar gradiometers, 102 magnetometers) whole-head VectorView MEG system (Elekta-Neuromag Ltd., Helsinki, Finland) in a magnetically shielded room. Vertical and horizontal electrooculogram (EOG) was recorded for detection of eye movements and blinks. The locations of anatomical landmarks (nasion and preauricular points), four head position indicator (HPI) coils, and additional points on the scalp were digitized for the co-registration of the MEG data with each subject's MRI. The three anatomical landmarks defined our head-based MEG coordinate system such that the x -axis passes through the two auricular points with positive direction to the right, the y -axis is perpendicular to the x -axis and passes through the nasion with positive direction to the front, and the positive z -axis points up (Fig. 3.1). Continuous MEG signals were sampled at 601 Hz after filtering from 0.03 to 200 Hz. Responses related to each stimulus condition were averaged offline using an epoch from -100 to 800 ms with

respect to the stimulus onset. Trials containing eye movements, blinks, or other channel artifacts (peak-to-peak amplitude $>150 \mu\text{V}$ in EOG or $>500 \text{ fT/cm}$ in gradiometers) were rejected. Averaged epochs were low-pass filtered with a cutoff at 40 Hz, and the zero level in each channel was taken to be the mean value in the 100-ms pre-stimulus baseline.

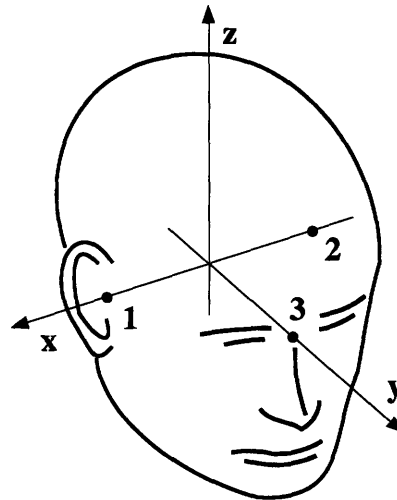


Figure 3.1: The coordinate system for the MEG measurements.

Auditory evoked MEG data was recorded as subjects performed an oddball detection task. Subjects were presented with 300 embedded deviant words (bat, cat, rat) in a train of 1000 standard word (pat) stimuli. The subjects were to press a button if they detected one of the deviants, and not to press a button otherwise. The experiment was divided into five four-minute sections or “runs” to give the subjects frequent breaks to rest. We analyzed the brain responses evoked by the standard word “pat”.

While recording MEG, continuous sinusoidal currents were fed to the four HPI coils positioned on the subject’s head. The position and orientation of the head with respect to the sensor array was computed at 200 ms intervals, using software provided by the MEG manufacturer. Using these data, the locations of the MEG sensors, originally given in a coordinate system fixed to the MEG device, were transformed to an

anatomically-based coordinate frame, which was defined by the digitized locations of fiducial landmarks on the head:

$$\mathbf{r}_h = \mathbf{T}\mathbf{r}_d \quad , \quad (1)$$

where $\mathbf{r}_h = [x_h \ y_h \ z_h \ 1]^T$ and $\mathbf{r}_d = [x_d \ y_d \ z_d \ 1]^T$ are the augmented location vectors in head-based and device-based coordinate system, respectively, and \mathbf{T} is the rigid body coordinate transformation matrix:

$$\mathbf{T} = \begin{bmatrix} \mathbf{R} & \mathbf{r}_0 \\ \mathbf{0} & 1 \end{bmatrix} \quad . \quad (2)$$

\mathbf{R} is the rotation matrix, and $\mathbf{r}_0 = [x_0 \ y_0 \ z_0]^T$ is the associated translation vector. We computed the mean displacement of the MEG sensors between the beginning of the experiment and each subsequent time point as

$$D(t) = \frac{1}{N_s} \sum_{k=1}^{N_s} \left\| \mathbf{r}_h^{(k)}(t) - \mathbf{r}_h^{(k)}(t_0) \right\| \quad , \quad (3)$$

where $\mathbf{r}_h^{(k)}(t)$ is the location of the k th sensor in head coordinates at time t and N_s is the number of sensors. In our case $N_s = 102$, since the Vectorview system has three separate sensors at the same location, we included only one of the sensors from each location in this calculation. To quantify the amount of head movement for each subject over time, the mean displacement and translation vectors were segmented into 10-second bins. In each time bin, we calculated the average and standard deviation of D , x_0 , y_0 , and z_0 .

3.2 Dipole localization error due to head movements

To investigate the effect of head movement on equivalent current dipoles, commonly used to model sources of MEG data, we simulated the magnetic fields from dipole sources and computed the error in the estimated dipole locations when the head movement was not taken into account. For each subject, high-resolution structural T1-weighted magnetic resonance images (MRIs) were acquired on a 3T Siemens Allegra or Trio head scanner (TR = 2530 ms, TE = 3.25 ms, flip angle = 7°, 128 slices, slice thickness = 1.3 mm, voxel size = 1.3 x 1.0 x 1.3 mm³). The MEG data was aligned with the MRI by using the digitized head shape information. A surface representation for the cerebral cortex was constructed using the FreeSurfer software (Dale, Fischl, & Sereno, 1999; Fischl, Sereno, & Dale, 1999). The cortical surface was decimated with spacing of about 5 mm between dipoles to yield approximately 7000 sources. A forward matrix \mathbf{A}_0 , where each column of which is the signal pattern generated by a unit dipole oriented normal to the cortical mantle at each selected location on the surface, was calculated for the initial head position using a boundary element model (BEM) representing the inner surface of the skull (Hämäläinen & Sarvas, 1989; Oostendorp & van Oosterom, 1989). Forward matrices $\mathbf{A}(t)$ were also calculated at one-second intervals using the sensor array position given by the HPI. The generated forward solutions were then treated as simulated data, and current dipoles were fitted to the field patterns corresponding to each dipole in the original forward solution and each of the transformed forward solutions. However, in all cases the sensor positions corresponding to the initial HPI measurement obtained from the beginning of the run was used in the fitting algorithm. No cortical location or orientation constraint was used in the fitting.

Our dipole fitting routine determined an initial guess for the ECD location by evaluating the least-squares error function in a volumetric grid within the cranial volume. This initial guess was refined with the non-linear Nelder-Mead simplex algorithm (Nelder & Mead, 1965) first using a spherically symmetric conductor model, then the boundary-element model, to find the final optimal dipole location.

The dipole fits to the original forward solution provided an estimate of the methodological error, whereas dipole fits to the transformed forward solutions provided information about the localization error if the head position data was not taken into account. Dipole localization error was calculated as the distance between the estimated and the actual source locations (Uutela et al., 2001). The mean and standard deviation of the localization error for each source location was calculated and displayed on an inflated cortical surface for five subjects.

3.3 Movement compensation using the Signal Space Separation method

The SSS method takes advantage of the oversampling of the measured magnetic field present in modern whole head MEG devices with many sensors (Taulu & Kajola, 2004). SSS represents the magnetic field as a truncated basis function expansion. Since the sensors in MEG systems are located in a source-free volume, the measured magnetic field can be expressed as the gradient of a harmonic scalar potential

$$\mathbf{B} = -\mu_0 \nabla V \quad . \quad (6)$$

This scalar potential can be expanded into a series as

$$V(\mathbf{r}) = \sum_{l=1}^{\infty} \sum_{m=-l}^l \alpha_{lm} \frac{Y_{lm}(\theta, \varphi)}{r^{l+1}} + \sum_{l=1}^{\infty} \sum_{m=-l}^l \beta_{lm} r^l Y_{lm}(\theta, \varphi) \quad , \quad (7)$$

where $Y_{lm}(\theta, \varphi)$ are the normalized spherical harmonic functions, α_{lm} and β_{lm} are scalar coefficients, and (r, θ, φ) are the spherical coordinates of the position vector \mathbf{r} . Importantly, the radial dependant part of the expansion separates into two sets of functions: those that are proportional to inverse powers of r and are singular at the origin [first term in Eq. (7)], and those that are proportional to powers of r and diverge at infinity [second term in Eq. (7)]. Any measured signal vector $\phi = [\phi_1, \dots, \phi_N]$ with measurements at N channels can be approximated as the truncated series

$$\phi = \sum_{l=1}^{L_{in}} \sum_{m=-l}^l \alpha_{lm} \mathbf{a}_{lm} + \sum_{l=1}^{L_{out}} \sum_{m=-l}^l \beta_{lm} \mathbf{b}_{lm} \quad , \quad (8)$$

where \mathbf{a}_{lm} and \mathbf{b}_{lm} are n -dimensional vectors containing the inside and outside basis functions respectively. In practice, the values $L_{in} = 8$ and $L_{out} = 3$ have been found to provide a faithful representation of the data (Taulu & Kajola, 2004). Eq. (8) can be written in compact matrix form

$$\phi = \mathbf{S}\mathbf{x} = \begin{bmatrix} \mathbf{S}_{in} & \mathbf{S}_{out} \end{bmatrix} \begin{bmatrix} \mathbf{x}_{in} \\ \mathbf{x}_{out} \end{bmatrix} \quad , \quad (9)$$

where

$$\mathbf{S}_{in} = [\mathbf{a}_{1,-1}, \dots, \mathbf{a}_{L_{in}L_{out}}], \mathbf{S}_{out} = [\mathbf{b}_{1,-1}, \dots, \mathbf{b}_{L_{in}L_{out}}], \mathbf{x}_{in} = [\alpha_{1,-1}, \dots, \alpha_{L_{in}L_{out}}]^T, \mathbf{x}_{out} = [\beta_{1,-1}, \dots, \beta_{L_{in}L_{out}}]^T.$$

A least-squares estimate $\hat{\mathbf{x}}$ is given by

$$\hat{\mathbf{x}} = \begin{bmatrix} \hat{\mathbf{x}}_{in} \\ \hat{\mathbf{x}}_{out} \end{bmatrix} = \mathbf{S}^\dagger \phi \quad , \quad (10)$$

where \mathbf{S}^\dagger is the pseudoinverse of \mathbf{S} . A reconstruction of the biomagnetic signals can then be performed by leaving out the contribution of sources external to the sensor array

$$\phi_{in} = \mathbf{S}_{in} \hat{\mathbf{x}}_{in} \quad . \quad (11)$$

The separation of sources inside the brain from those outside of the sensor array allows for the suppression of external interference signals such as heartbeat artifacts in MEG data collected from children and infants (Cheour et al., 2004; Pihko et al., 2004).

Of particular interest to the present study is that SSS can be used to extrapolate the measured signals from different head positions to a virtual array that is fixed with respect to the subject's head (Taulu, Simola, & Kajola, 2005). One way to accomplish this is to average the estimated coefficients, \hat{x} , generated for each data epoch, rather than averaging epochs directly from the raw data. This approach requires the calculation of a pseudoinverse for each epoch, and therefore can be quite time consuming. A faster method is to simply use the raw data averaged over all epochs with the SSS basis averaged over all head positions, updated in our case every 200 ms, to generate the virtual signals corresponding to a desired reference head position (Taulu & Kajola, 2004).

Previously, simulations and a study with infants have been performed to test the applicability of SSS for use as an effective movement compensation method (Cheour et al., 2004; Taulu et al., 2005). However, the SSS method has not been evaluated in children performing a typical cognitive task. Here we provide such an evaluation by comparing the results obtained by the SSS correction with results obtained using the forward solution correction method discussed by Uutela and colleagues (Uutela et al., 2001).

We evaluated the effect of head movements on two different source estimates, ECD and MNE, of the magnetic N100 response (N100m) to the repeated stimulus "pat". To quantify the effect of SSS-compensation on ECD localization, a single dipole was fit at the peak of the N100m response in each hemisphere with and without SSS movement

compensation using a spherical source model with head origin at $x = y = 0$ mm, $z = 40$ mm. The N100m is an obligatory response to auditory stimuli (Näätänen & Picton, 1987), and its neural generators are expected to remain relatively constant across trials. Generators of the N100m have been localized to the supra-temporal plane within Heschl's gyri (Reite et al., 1994). However, we expected to observe spatial smearing of the magnetic field pattern due to the head movements, which would result in a lower goodness-of-fit for the ECDs. The goodness-of-fit is defined as

$$g = 1 - \frac{(\phi - \hat{\phi})^T (\phi - \hat{\phi})}{\phi^T \phi}, \quad (12)$$

where ϕ and $\hat{\phi}$ are measured and model signal vectors, respectively. We hypothesized that a reduction in spatial variance when SSS was applied would lead to an increase in the goodness-of-fit of the ECD compared to when SSS was not applied. The Wilcoxon signed-rank test was used to determine significant differences between the SSS-corrected and uncorrected data for ECDs fit to each hemisphere of all twenty subjects.

In addition to the goodness-of-fit measure, we examined the effect of the SSS compensation on the confidence limits of the ECD location using a bootstrap method (Darvas et al., 2005). Data from two runs of a single subject were used: one with minimal head movement, and one with considerable movement. The data were averaged and noisy epochs were rejected, giving approximately $n = 100$ trials of the standard stimulus “pat” in each run. Two hundred bootstrap samples were generated by randomly selecting and averaging n epochs from the raw data (with replacement); noisy epochs were excluded from the analysis. A single dipole was fit at the peak of the N100m response to each bootstrap sample, with and without SSS movement compensation. This resulted in two clusters of dipoles (one with and one without SSS-compensation) for each

of the two runs. We hypothesized that the application of SSS should reduce the variance in the ECD locations caused by the head movement. To quantify this variance, we calculated confidence volumes for each dipole cluster. The dipole locations $\mathbf{r}_1, \dots, \mathbf{r}_{200}$ were transformed to the center of mass, and the principle axes of the confidence volume ellipsoid were calculated using the singular value decomposition

$$(\mathbf{r}_1, \dots, \mathbf{r}_{200}) = U\Omega V^T, \quad (13)$$

where U and V^T are unitary matrices and $\Omega = \text{diag}(\lambda_1, \lambda_2, \lambda_3)$, with $\lambda_1, \lambda_2, \lambda_3$ as the singular values. The values $\lambda_1, \lambda_2, \lambda_3$ were converted into standard deviations as

$$\sigma = \lambda / \sqrt{m-1}, \quad (14)$$

where m is the number of bootstrap resamples; in our case $m = 200$. Assuming a Gaussian distribution for the dipole clusters, a 95% confidence interval along each axis of the ellipsoid was calculated as $\pm 2\sigma = 4\sigma$. The 95% confidence volumes for each dipole cluster were then calculated as $4^3(\sigma_1\sigma_2\sigma_3)$.

We also examined the effect of SSS head motion compensation on a distributed source estimate, the minimum norm estimate (MNE) (Hämäläinen & Ilmoniemi, 1994). The MNE was calculated by constructing a linear inverse operator $\mathbf{A}^T(\mathbf{A}\mathbf{A}^T + \gamma\mathbf{C})^{-1}$, where \mathbf{A} is the forward matrix, \mathbf{C} is the noise covariance matrix, and γ is a regularization parameter. In the cortically-constrained MNE, the underlying sources of the MEG signals are assumed to lie on the cortical surface, constructed for each subject. The same dipole locations and orientations that were generated for the dipole simulations were also used for calculating the distributed MNE solution. One method that has previously been used to compensate for small head movements between runs is to average the forward solutions for each run separately using the initial head position measurement for that run

(Uutela et al., 2001). While this method appears to work well for adults who tend to have minimal head movement throughout the experiment, it neglects head movement during each run. However, for some children, there appears to be considerable intra-run movement. To assess the impact of SSS on MNE localization we computed the forward solution under four different conditions: (1) the initial head position from run 1 only, (2) the average forward solution which takes into account the initial head position at the beginning of each run, (3) SSS-correction where the data for each run was transformed to the head position at the beginning of that run, and (4) SSS-correction where the data for each run was transformed to the head position at the beginning of the experiment. The difference between these conditions was quantified with paired *t*-test comparisons by determining the mean MNE amplitude difference within a small cortical patch surrounding the MEG response corresponding to the peak N100m response in each hemisphere for the four forward solution conditions. One subject was excluded from the statistical comparisons due to a large amount (> 20 mm) of inter-run movement.

We hypothesized that compensating for the head movements would result in a larger amplitude of the MNE response corresponding to the N100m due to the decrease in spatial smearing of the MEG signals.

4. Results and Discussion

4.1 Quantitative assessment of head movement in children

Head movement statistics for one child performing a simple cognitive task during an MEG recording is plotted in Fig. 4.1. The movement was largest in the z (up/down) direction, and increased toward the end of the experiment. On average, the displacement of the head from the position at the beginning of the experiment was 12 mm (range: 3-26 mm) across 19 subjects. The average standard deviation was 3.7 mm in the x -direction, 15 mm in the y -direction, and 23 mm in the z -direction. A planned series of paired t -tests comparing the magnitude and variance of head movement in each direction (e.g., x -direction vs. y -direction) indicated that there was more variation in head movement for the z -direction than the x - and y -directions ($p < 0.01$, and $p < 0.05$ respectively), and more variation in head movement in the y -direction than the x -direction ($p < 0.01$).

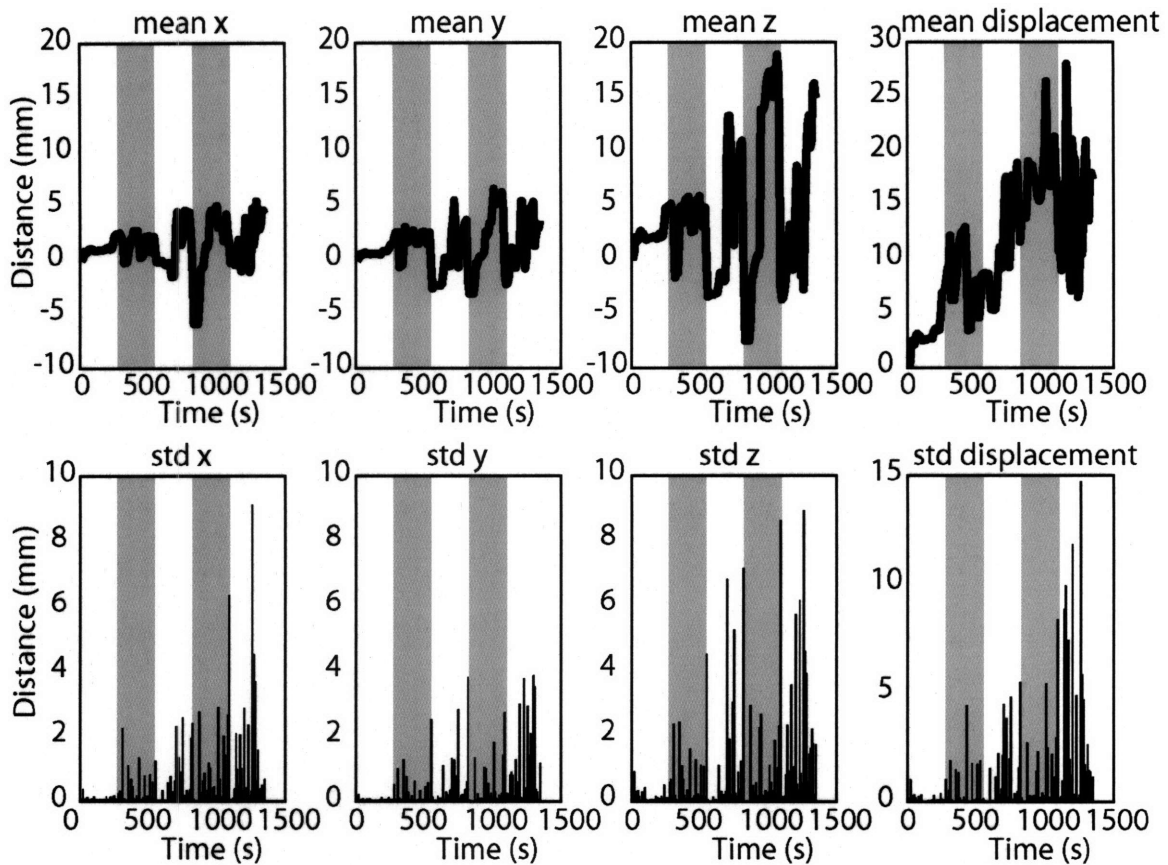


Figure 4.1: The mean (top) and standard deviation (bottom) head movement in 10-second bins for one child over the course of the entire 25-minute experiment. The left three columns describe the relative head movement in the x (right-left), y (front-back), and z (up-down) directions, whereas the rightmost column indicates the absolute amount of head movement relative to the head position at the beginning of the experiment. The five runs are indicated with the alternating unshaded/shaded intervals.

A likely explanation for the movement to be largest in the z -direction (up/down) is that over the course of the experiment, most subjects begin to slouch in the seat, thereby lowering their head in the measurement helmet. Although a particularly salient problem for children, this downward movement has also been seen in adults (Wehner,

unpublished data). One way to avoid the downward movement of the head is to record MEG data the supine position. However, this is often less comfortable for the subject, especially if EEG electrodes are attached on the scalp. The second largest head movements were in the y -direction (front/back). As a child's head is smaller than the inside of the helmet containing the measurement sensors, there is ample opportunity for front/back head movement should the child sneeze, cough, or simply lean forward/back. Different positioning of the head in the front/back direction with respect to the MEG sensor array has been shown to strongly affect the detection of frontal activity in adults (Marinkovic et al., 2004); the effect is expected to be even larger in children. The amount of empty space on the sides of the head is usually less, reflected in the smallest head movements in the x -direction (side-to-side). Rotations of the head, particularly “nodding” the head forward and downward as sometimes happens when the subject is tiring, would also show head movement in the y - and z -directions but not in the x -direction. Overall, the results indicate that a considerable amount of head motion occurs over the course of a typical 25-minute MEG experiment with children. In the next section we will examine the effect of this head movement on source estimation.

4.2 Dipole localization error due to head movements

The effect of realistic head motion on the localization error of dipoles distributed throughout the cortex was examined using dipole simulations. The locations of the sources used in the simulations are shown in Fig. 4.2A for one subject. The cortical distribution of the localization error introduced by the dipole fitting method in the absence of noise or head movement is shown in Fig. 4.2B. The automated dipole-fitting

algorithm that was used in the simulations was able to localize the majority of sources precisely in the ideal case, i.e., without movement or noise. Histograms of the dipole localization errors across five subjects, shown on the right side of Fig. 4.2B, indicates that most of the localization errors were below 5 mm. The locations with the largest localization errors were typically located deep in the sulci, evidenced by the larger number of mislocated sources on the medial surface of both hemispheres. Inclusion of simulated EEG data in combination with the MEG data could help to lower this methodological error in these problematic locations. The effect that head motion had on the dipole localization errors throughout the cortex is shown in Figs. 4.2C and 4.2D. With minimal head movement (Fig. 4.2C), the mean localization errors were only slightly larger than seen in the ideal case (Fig. 4.2B). However, when there was a considerable amount of movement, the mean localization error was about 12 mm (Fig. 4.2D).

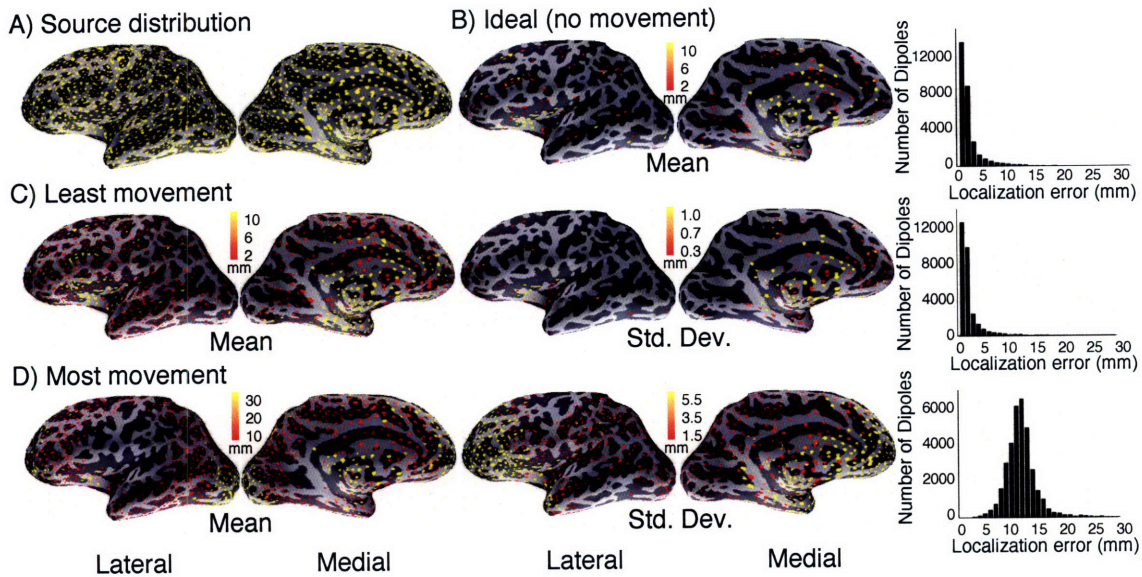


Figure 4.2: Dipole source localization errors A) Sources used in the simulations are shown (yellow dots) on inflated cortical surfaces of the left hemisphere for one subject. B) Dipole sources that had a localization error larger than 2 mm in the absence of noise and head movements using the automated dipole fitting procedure. The amount of localization error is indicated by the color scale. The histogram shows group data (5 subjects) indicating the total number of dipoles with different localization errors. C) Dipole localization errors in a five-minute run with small head movements. Left: mean and standard deviation in a single subject. Right: Histogram of group data (5 subjects). D) Dipole localization errors in a five-minute run with large head movements.

The largest localization errors that were induced by the head movement in the subject shown in Fig. 4.2 reside along the inferior and superior borders of the head in

both hemispheres, and regions in the frontal and occipital cortices. This could result from the subject rotating their head forward and down during the course of the experiment. In such a case, the points on the head with the most movement would correspond to those farthest from the center of rotation. Similarly, if the head were to rotate around the vertical axis (e.g., from side to side), the locations on the head with the most movement would be points on the inferior and superior surface of the head as well as those in the frontal and occipital cortices.

The dipole localization error due to the head movement was of the same order of magnitude than errors previously reported due to other sources of uncertainty, including measurement noise (Hari, Joutsiniemi, & Sarvas, 1988; Mosher, Spencer, Leahy, & Lewis, 1993) and forward modeling (Cohen et al., 1990; Cuffin, 1990; Leahy, Mosher, Spencer, Huang, & Lewine, 1998). Therefore, head movement compensation methods can potentially improve the quality of MEG recordings and reduce the error in source estimates.

4.3 Movement compensation using the Signal Space Separation method

SSS movement compensation was applied to the data in two ways (Fig. 4.3). First, SSS was applied only within runs, thereby transforming all measurements within a run to the head position measured at the beginning of that run. The data from each of the corrected runs was then averaged to produce the result seen in Fig. 4.3 (blue traces). Second, all measurements were transformed with SSS to the head position measured at the beginning of the experiment, rather than at the beginning of each run. The data was then averaged across runs to produce the result in Fig. 4.3 (green traces).

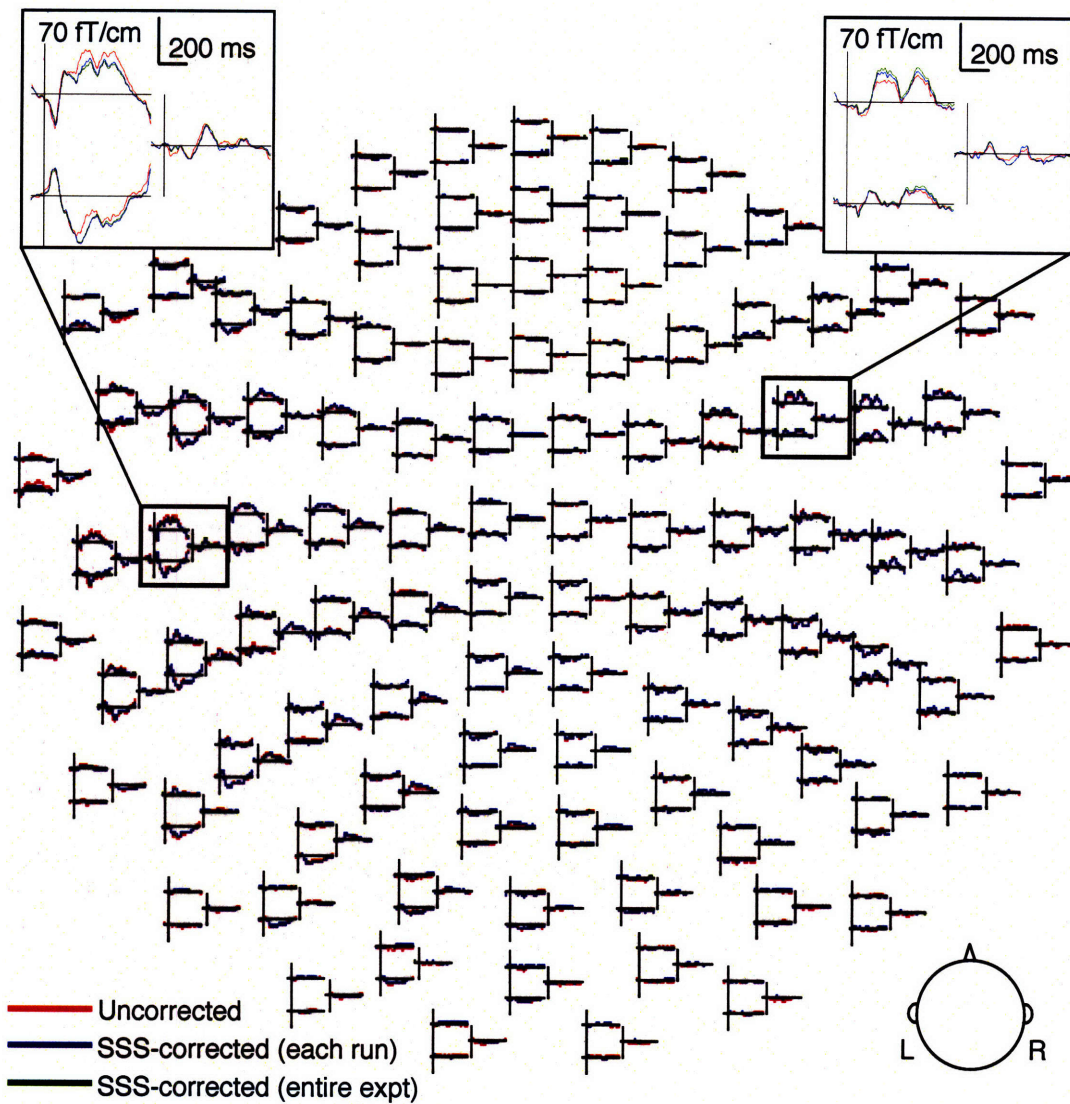


Figure 4.3: Event-related magnetic fields for one child. The averaged responses in the uncorrected, SSS-corrected (each run), and SSS-corrected (entire experiment) conditions are superimposed. The spatial distribution of the signal waveforms in 204 gradiometer and 102 magnetometer sensors is shown (L: left hemisphere, R: right).

4.3.1 Equivalent Current Dipoles

To quantify the change in ECD location across all subjects, we calculated the mean change (SSS corrected – uncorrected) in the location and goodness of fit for N100m dipole sources fit to each hemisphere. On average the change in location was 5.0 mm in the left hemisphere, and 5.6 mm in the right hemisphere. It was difficult to determine if the ECD localization after SSS correction was more or less accurate than without correction because of our lack of knowledge about the true source location using this method. The ECD goodness of fit increased after SSS-correction for 15/20 subjects in the left hemisphere and 14/20 subjects in the right hemisphere. For the group, the average change in ECD goodness-of-fit was 1.5% for the left hemisphere and 1.0% for the right hemisphere. Significant differences between the ECD goodness of fits for the corrected and uncorrected data were evaluated with Wilcoxon signed-rank tests. After the SSS-correction, the ECD goodness of fit was significantly greater for the left hemisphere ECDs ($p < 0.01$), but not for the right hemisphere ECDs ($p > 0.1$).

A bootstrap approach was applied to ECDs fit to the N100m response in one subject; we only examined the clusters in the right hemisphere, which showed stronger signals in this subject. In the run with the least amount of movement (mean displacement from beginning of run: 2.7 mm), uncorrected: $\sigma_1 = 2.1$ mm, $\sigma_2 = 1.7$ mm, $\sigma_3 = 1.2$ mm, confidence volume = 274 mm³, SSS-corrected: $\sigma_1 = 2.2$ mm, $\sigma_2 = 1.7$ mm, $\sigma_3 = 1.3$ mm, confidence volume = 311 mm³. In the run with the most movement (mean displacement from beginning of run: 17.5 mm), uncorrected: $\sigma_1 = 3.3$ mm, $\sigma_2 = 2.8$ mm, $\sigma_3 = 2.1$ mm, confidence volume = 1240 mm³, SSS-corrected: $\sigma_1 = 3.2$ mm, $\sigma_2 = 2.6$ mm, $\sigma_3 = 1.9$ mm,

confidence volume = 1010 mm³. Therefore, with SSS compensation, the 95% confidence volume was reduced in the run with the most movement.

4.3.2 Minimum Norm Estimates

To assess the impact of SSS on the distributed source estimate, MNE, we examined four different levels of movement compensation: (1) no compensation, using the initial head position from run 1 only, (2) the average forward solution that takes into account the initial head position at the beginning of each run, (3) SSS-corrected data for each run, transformed to the head position at the beginning of that run, and (4) SSS-corrected data for each run, transformed to the head position at the beginning of the experiment. The location of the activation was similar across the different forward-solution conditions. The MNE maps for the N100m response suggest that the estimated source amplitudes were larger when increasing amounts of information about the head position was taken into account (Fig. 4.4).

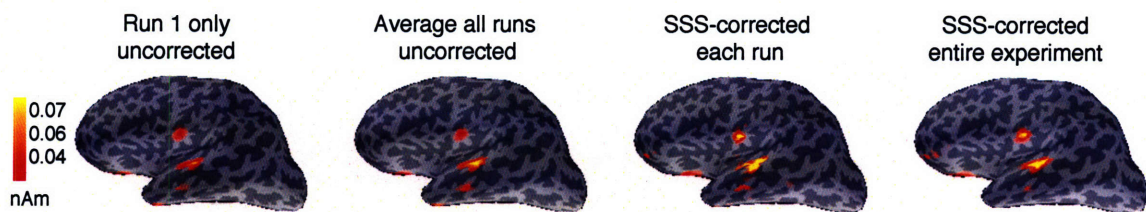


Figure 4.4: Minimum Norm Estimates at the peak latency of the N100m in one child. The estimates were calculated using four different forward solutions.

The mean MNE amplitude within a cortical patch representing the left hemisphere N100m response for each of the four conditions for one subject is shown in Fig. 4.5A.

Group data representing the peak MNE response across all subjects for each of the four conditions is shown in Fig. 4.5B.

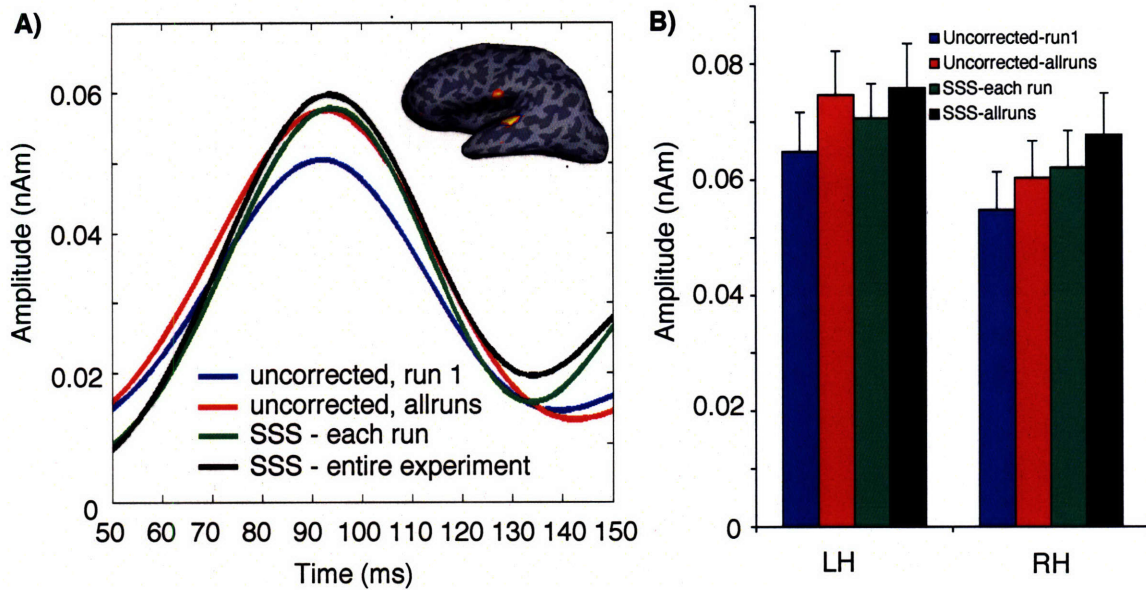


Figure 4.5: The effect of SSS compensation on Minimum Norm Estimates (MNE). A) The N100m MNE response in the left hemisphere of one subject. The patch of cortex that was used for comparison of the different forward-solution conditions is outlined in blue. B) Group data ($n=19$) for the peak MNE response in the left hemisphere (LH) and right hemisphere (RH) region.

The cortical location corresponding to the peak N100m response and the magnitude of the MNE response for a small patch of cortex surrounding the peak response was determined for each subject and condition. A series of pairwise t -tests indicated that the peak N100m response in the left hemisphere was significantly larger for all three conditions (uncorrected, all runs; SSS, each run; SSS, entire experiment) relative to the peak N100m amplitude for the uncorrected-run1 condition ($p < 0.01$, $p <$

0.09, and $p < 0.03$ for the three conditions respectively). There was a trend ($p = 0.14$) toward larger N100m amplitudes for the SSS-each run condition relative to the uncorrected-allruns condition, although this difference was not significant. There was a significant difference ($p < 0.04$) however in the peak N100m amplitudes for the two SSS methods, with larger amplitudes for the SSS-entire experiment condition relative to the SSS-each run condition. The right hemisphere peak N100m responses again yielded significantly larger amplitudes for the three tested conditions ($p < 0.02$, $p < 0.01$, $p < 0.02$, respectively) relative to the uncorrected-SSS method. In addition, there were significantly larger N100m amplitudes for the SSS-entire experiment condition compared to the SSS-each run condition ($p < 0.04$) and the uncorrected-allruns condition ($p < 0.04$).

4.4 Discussion

We found that applying SSS movement compensation to the MEG data improved the source estimates: the goodness-of-fit of ECDs was higher, the estimated confidence limits for ECD locations were smaller, and the amplitude of the distributed source estimates were enhanced after SSS compensation. The results suggest that SSS sharpened the spatial pattern of the measured signals, thereby successfully compensating for the spatial smoothing cause by head movement during the MEG recordings.

For ECD goodness-of-fit, the spatial smoothing due to head movements changes the spatial pattern of the averaged MEG signals such that the pattern cannot be explained with a single ECD, even if the true brain source were focal, and could be well modeled with a dipole in the absence of head movement. For confidence limits, head movement can be considered as an effective increase in the measurement noise, and therefore, the

movement increased the uncertainty in the ECD parameters estimated from the data. The amplitude of MNE was found to be smaller when less head movement data was taken into account, partly due to the reduction in peak amplitudes in the spatial signal patterns, and partly due to smoothing of the signal patterns resulting in spatially smoothed source estimates.

It is evident from Fig. 4.5B that the N100m-related activation was enhanced as more information was taken into account. Our results have also indicated that as a first step, averaging the forward solutions from several runs gives a more robust signal compared to using the forward solution from a single run (Uutela et al., 2001). The application of SSS to each run, and to the entire experiment helped to further sharpen the N100m response. Sharpening of the response resulting in higher effective signal-to-noise ratio (SNR) may be crucial for some cognitive experiments with children if the choice of stimuli and/or the attention of the child is limited. The higher SNR would allow for the use of less stimuli and shorter experiments.

5. Conclusions

5.1 Summary

The application of SSS to MEG data appears to be an effective way of compensating for head movements in children during MEG recordings. Although the best method of controlling for head movement is to tell the child to hold as still as possible, inevitably the child's head will move over the course of the experiment. We have quantified for the first time the amount and direction of natural head movements of 8-12 year-old children while they perform a typical cognitive task in MEG. Although all children were instructed to remain as still as possible during the measurement, mean head position displacement from the beginning of the experiment ranged from 3-26 mm. By monitoring the head position continuously throughout the experiment, we were able to determine that the largest variation in movement was in the z -direction (up/down). Dipole simulations have helped us to illustrate that the inferior and superior borders of the brain and the frontal cortex are particularly sensitive to head movements. Future studies that do not take head movements into account may need to consider if spatial smearing of the magnetic field patterns during the averaging process may be a possible cause of the small activations observed in these regions.

Application of SSS for movement compensation was evaluated using ECD and MNE source modeling. The SSS correction sharpened the MEG responses by reducing the spatial smearing of the MEG signals that was introduced by the movement. For the ECD analysis, the goodness-of-fit of dipoles was increased in the majority of subjects, and SSS reduced the confidence volumes of dipole clusters in a single subject. Similarly, the MNE analysis showed that the SSS-correction produced N100m responses that were

larger than for the uncorrected condition. Based on the results of this study, it appears that SSS is an effective method to compensate for natural head movements in MEG data recorded in children.

5.2 Future Work

Application of SSS to the MEG data provided moderate gains in SNR by the reduction of the spatial smoothing of the MEG signals due to head movements. Despite telling the subjects to keep still during the measurement, a large amount of head movements occurred in some children. Further studies are necessary to understand why the differences between uncorrected and SSS-corrected data, while significant, were smaller than anticipated. One possible explanation may have been that some of the children's heads were far from the sensor array, and thus there was a low SNR to begin with. While SSS can increase the SNR by reducing the spatial noise, the method cannot recover signals that were not detected. If the relative size of the spatial noise introduced by the head movements was small compared to other types of noise in the recording, then SSS-compensation may not do much to improve the data quality. Additionally our use of speech stimuli may have elicited smaller signals than less complex stimuli (e.g., tones).

Bibliography

- Ahlfors, S., & Ilmoniemi, R. (1989). Magnetometer position indicator for multichannel MEG. In S. J. Williamson, M. Hoke, G. Stroink & M. Kotani (Eds.), *Advances in Biomagnetism* (pp. 693-696). New York: Plenum.
- Burghoff, M., Nenonen, J., Trahms, L., & Katila, T. (2000). Conversion of magnetocardiographic recordings between two different multichannel SQUID devices. *IEEE Transactions on Biomedical Engineering*, *47*, 869-875.
- Cheour, M., Imada, T., Taulu, S., Ahonen, A., Salonen, J., & Kuhl, P. (2004). Magnetoencephalography is feasible for infant assessment of auditory discrimination. *Experimental Neurology*, *190 Supplement 1*, S44-51.
- Cohen, D. (1972). Magnetoencephalography: detection of the brain's electrical activity with a superconducting magnetometer. *Science*, *175*, 664-666.
- Cohen, D. (1999). Magnetoencephalography (neuromagnetism). In G. Adelman & B. H. Smith (Eds.), *Elsevier's Encyclopedia of Neuroscience* (2nd enlarged and revised edition ed., pp. 1079-1083): Elsevier Science B.V.
- Cohen, D., Cuffin, B. N., Yunokuchi, K., Maniewski, R., Purcell, C., Cosgrove, G. R., Ives, J., Kennedy, J. G., & Schomer, D. L. (1990). MEG versus EEG localization test using implanted sources in the human brain. *Annals of Neurology*, *28*, 811-817.
- Cuffin, B. N. (1990). Effects of head shape on EEG's and MEG's. *IEEE Transactions on Biomedical Engineering*, *37*, 44-52.
- Dale, A. M., Fischl, B., & Sereno, M. I. (1999). Cortical surface-based analysis. I. Segmentation and surface reconstruction. *Neuroimage*, *9*, 179-194.
- Darvas, F., Rautiainen, M., Pantazis, D., Baillet, S., Benali, H., Mosher, J. C., Garnero, L., & Leahy, R. M. (2005). Investigations of dipole localization accuracy in MEG using the bootstrap. *Neuroimage*, *25*, 355-368.
- de Munck, J. C., Verbunt, J. P., Van't Ent, D., & Van Dijk, B. W. (2001). The use of an MEG device as 3D digitizer and motion monitoring system. *Physics in Medicine and Biology*, *46*, 2041-2052.
- Fischl, B., Sereno, M. I., & Dale, A. M. (1999). Cortical surface-based analysis. II: Inflation, flattening, and a surface-based coordinate system. *Neuroimage*, *9*, 195-207.
- Fuchs, M., Wischmann, H. A., Wagner, M., & Kruger, J. (1995). Coordinate system matching for neuromagnetic and morphological reconstruction overlay. *IEEE Transactions on Biomedical Engineering*, *42*, 416-420.
- Hämäläinen, M. S., Hari, R., Ilmoniemi, R., Knuutila, J., & Lounasmaa, O. V. (1993). Magnetoencephalography - theory, instrumentation, and applications to noninvasive studies of the working human brain. *Reviews of Modern Physics*, *65*, 413-497.
- Hämäläinen, M. S., & Ilmoniemi, R. J. (1994). Interpreting magnetic fields of the brain: minimum norm estimates. *Medical and Biological Engineering and Computing*, *32*, 35-42.
- Hämäläinen, M. S., & Sarvas, J. (1989). Realistic conductivity geometry model of the human head for interpretation of neuromagnetic data. *IEEE Transactions on Biomedical Engineering*, *36*, 165-171.

- Hamilton, W. R. (1853). *Lectures on Quaternions: Containing a Systematic Statement of a New Mathematical Method*. Dublin: Hodges and Smith.
- Hari, R., Joutsiniemi, S. L., & Sarvas, J. (1988). Spatial resolution of neuromagnetic records: theoretical calculations in a spherical model. *Electroencephalography and Clinical Neurophysiology*, *71*, 64-72.
- Incardona, F., Narici, L., Modena, I., & Erne, S. N. (1992). Three-dimensional localization system for small magnetic dipoles. *Reviews of Scientific Instrumentation*, *63*, 4161-4166.
- Leahy, R. M., Mosher, J. C., Spencer, M. E., Huang, M. X., & Lewine, J. D. (1998). A study of dipole localization accuracy for MEG and EEG using a human skull phantom. *Electroencephalography and Clinical Neurophysiology*, *107*, 159-173.
- Marinkovic, K., Cox, B., Reid, K., & Halgren, E. (2004). Head position in the MEG helmet affects the sensitivity to anterior sources. *Neurology and Clinical Neurophysiology*, *2004*, 30.
- Mosher, J. C., Spencer, M. E., Leahy, R. M., & Lewis, P. S. (1993). Error bounds for EEG and MEG dipole source localization. *Electroencephalography and Clinical Neurophysiology*, *86*, 303-321.
- Näätänen, R., & Picton, T. (1987). The N1 wave of the human electric and magnetic response to sound: a review and an analysis of the component structure. *Psychophysiology*, *24*, 375-425.
- Nelder, J. A., & Mead, R. (1965). A Simplex Method for Function Minimization. *Computer Journal*, 308-313.
- Numminen, J., Ahlfors, S., Ilmoniemi, R., Montonen, J., & Nenonen, J. (1995). Transformation of multichannel magnetocardiographic signals to standard grid form. *IEEE Transactions on Biomedical Engineering*, *42*, 72-78.
- Oostendorp, T. F., & van Oosterom, A. (1989). Source parameter estimation in inhomogeneous volume conductors of arbitrary shape. *IEEE Transactions on Biomedical Engineering*, *36*, 382-391.
- Paetau, R. (2002). Magnetoencephalography in pediatric neuroimaging. *Developmental Science*, *5*, 361-370.
- Phillips, C. (2005). Electrophysiology in the study of developmental language impairments: Prospects and challenges for a top-down approach. *Applied Psycholinguistics*, *26*, 79-96.
- Pihko, E., Lauronen, L., Wikstrom, H., Taulu, S., Nurminen, J., Kivitie-Kallio, S., & Okada, Y. (2004). Somatosensory evoked potentials and magnetic fields elicited by tactile stimulation of the hand during active and quiet sleep in newborns. *Clinical Neurophysiology*, *115*, 448-455.
- Reite, M., Adams, M., Simon, J., Teale, P., Sheeder, J., Richardson, D., & Grabbe, R. (1994). Auditory M100 component 1: relationship to Heschl's gyri. *Brain Research: Cognitive Brain Research*, *2*, 13-20.
- Sarvas, J. (1987). Basic mathematical and electromagnetic concepts of the biomagnetic inverse problem. *Physics in Medicine and Biology*, *32*, 11-22.
- Sato, S., Balish, M., & Muratore, R. (1991). Principles of magnetoencephalography. *Journal of Clinical Neurophysiology*, *8*, 144-156.
- Taulu, S., & Kajola, M. (2004). Presentation of electromagnetic data: The signal space separation method. *Journal of Applied Physics*, *97*.

- Taulu, S., Simola, J., & Kajola, M. (2005). Applications of the Signal Space Separation Method. *IEEE Transactions on Signal Processing*, *53*, 3359-3372.
- Uutela, K., Taulu, S., & Hämäläinen, M. (2001). Detecting and correcting for head movements in neuromagnetic measurements. *Neuroimage*, *14*, 1424-1431.
- Wilson, H. S. (2004). Continuous head-localization and data correction in a whole-cortex MEG sensor. *Neurology and Clinical Neurophysiology*, *2004*, 56.
- Zimmerman, J. E., Thiene, P., & Harding, J. T. (1970). Design and operation of stable rf-biased superconducting point-contact quantum devices and a note on the properties of perfectly clean metal contacts. *Journal of Applied Physics*, *41*, 1572-1580.